PCCP

PAPER

View Article Online
View Journal | View Issue

Cite this: *Phys. Chem. Chem. Phys.*, 2018, **20**, 4351

Molecular electrostatic potential on the proton-donating atom as a theoretical descriptor of excited state acidity†

Yu-Fu Wang and Yuan-Chung Cheng *

Organic photoacids with enhanced acidities in the excited states have received much attention both experimentally and theoretically because of their applications in nanotechnology and chemistry. In this study, we investigate the excited-state acidities of 14 hydroxyl-substituted aromatic photoacids, with a focus on using theoretical molecular electrostatic potential (MEP) as an effective descriptor for photoacidity. For these model photoacids, we applied time-dependent density functional theory (TDDFT) at the ωB97X-D/6-31G(d) level to calculate the molecular electrostatic potentials of S_1 excited states and show that the molecular electrostatic potential on the proton-donating atom exhibits a linear relationship with the observed excited-state logarithmic acid dissociation constant (pK_a^*). As a result, the molecular electrostatic potential on the proton-donating atom can be used to estimate the pK_a^* values based on simple TDDFT calculations for a broad range of hydroxyl-substituted aromatic compounds. Furthermore, we explore the molecular electrostatic potential as a quantum descriptor for the photoacidities of cationic photoacids, and show a universal behavior of the pK_a^*–MEP dependence. We also investigate the solvent effects on the photoacidity using TDDFT calculations with implicit solvent models. Finally, we discuss the physical insights implicated by the molecular electrostatic potential as a successful measure for photoacidity on the mechanism of proton transfer in the molecular excited states. This pK_a^* descriptor provides an effective means to quantify the tendency of excited-state proton transfer with a relatively small computational cost, which is expected to be useful in the design of functional photoacids.

Received 27th March 2017,
Accepted 3rd January 2018

DOI: 10.1039/c7cp01948c

rsc.li/pccp

1 Introduction

Organic photoacids are compounds with enhanced acidity in the excited state.[1–5] Combined with controlled photoexcitation by using laser lights, photoacids allow temporal and spatial pH control in condensed-phase environments. As a result, photoacids have received considerable attention both experimentally and theoretically. For example, photoacids play important roles in photo-initiated polymerization catalysts,[6,7] photolithography,[8] and even in novel drug-delivery systems.[9] In particular, hydroxyl-substituted aromatic molecules, such as phenol derivatives,[2,10–13] naphthol derivatives,[2,14,15] hydroxypyrene structures[14] and additional heteroaromatic molecules,[16] have been investigated for their excited state acidities. The acidities of these compounds are generally enhanced upon photoexcitation, with strong tendencies for excited state proton transfer (ESPT) to take place.[14,17,18] To understand the mechanism of ESPT and to quantitatively treat these photoacids in chemical reactions, interests arise in developing an efficient estimation of their excited-state logarithmic acid dissociation constant, pK_a^*, either by experiments or theoretical calculations.

Experimentally, fluorescence titration and the thermodynamic Förster cycle[19] are often applied to measure photoacidity.[1,2] In principle, the fluorescence of photo-excited species can be measured as a function of pH,[12] and the intensity of the characteristic emission may reflect the degrees of dissociation to yield the magnitude of the excited-state pK_a (pK_a^*). Additionally, based on the Förster cycle,[19–21] one can utilize the peak positions of the ultraviolet absorption spectrum to obtain the free energy difference between the excited state and the ground state of either the protonated or the deprotonated species. With the combination of the ground state pK_a value and the excitation free energy of each species, the excited-state pK_a^* value can be calculated. In practice, these experiments are often complicated by factors such as spectral congestion or contamination of impurities in the samples, and an accurate measurement of pK_a^* values is often a challenging task.

Theoretically, accurate determination of pK_a values in condensed-phase systems based on the thermodynamic Förster

---

Department of Chemistry, National Taiwan University, Taipei City 106, Taiwan. E-mail: yuanchung@ntu.edu.tw

† Electronic supplementary information (ESI) available. See DOI: 10.1039/c7cp01948c

cycle entails a significant challenge even for ground-state systems, because the procedure requires the calculations of free energies. As a result, much effort has been devoted to seek molecular proxies that can be used to efficiently determine molecular acidities, and many descriptors have been proposed for ground state systems. For example, the linear relationships between the ground-state pK_a values and specific C–O bond lengths in the crystal structures of a broad range of organic acids were reported previously and used as an acidity descriptor by several groups.[22–24] Based on semi-empirical quantum-mechanical methods, Tehan *et al.*[25] have shown that the properties derived from frontier electron theory, especially the electrophilic superdelocalizability (SE), exhibit a strong correlation with the pK_a values for a large number of compounds. Furthermore, by applying the "Atoms in Molecules (AIM)" theory, quantum structure–activity relationships (QSAR) have been developed[26] to describe the molecular acidity. These estimations based on the quantum topological molecular similarity (QTMS)[27] performed well in predicting the properties dominated by electronic effects, including pK_a. Besides, additional molecular properties such as the energy of the highest occupied molecular orbital (HOMO),[28] the atomic partial charge,[29] the proton dissociation energy,[30] and the molecular quantum self-similarity measurements (MQS-SM)[31] were also demonstrated to be related to molecular pK_a when applied to a specific group of compounds. Nevertheless, although these descriptors successfully provide a relationship for the estimation of molecular acidities in the ground states, they are often system specific and the correlations between these properties and the strength of the excited state acidities have not been investigated before.

Recently, Liu and Pedersen[32] have shown a strong correlation between the ground state acidities and the molecular electrostatic potential (MEP) on the proton-donating atom. They compared the experimental pK_a values of a large database of –OH, –NH, and –SH substituted compounds and the MEP calculated using *ab initio* density functional theory (DFT) to reveal a general linear correlation between pK_a and the difference between the MEP on the proton-donating atom in a molecule and that of the atom in the neutral atomic state. As a result they demonstrated an efficient quantum descriptor for molecular acidity based on simple DFT calculations. The idea of utilizing the electrostatic potential to report on the acidity and the resulting universal quantum descriptor for molecular pK_a values are remarkable as well as physically insightful, because the strong correlation between the MEP on the proton-donating atom and molecular acidity can be linked to a microscopic picture of the electrostatic control of proton transfer.[32] We believe that the same physical concept can be applied to excited states as well. It will be valuable if this correlation between the acidity and MEP can be generalized to excited-state systems to predict the excited-state pK_a values (pK_a*) for photoacids.

In this work, we investigate the excited-state acidities of a series of hydroxyl-substituted aromatic photoacids. We utilize time dependent density functional theory (TDDFT) to calculate the optimized geometries of the S_1 excited states and the electrostatic potentials on the proton-donating atom of these compounds, and examine the correlation between the experimentally measured pK_a* values and the MEPs on the proton-donating atom. To investigate the solvent effects, we also carry out calculations using implicit solvent models. We aim to reveal the factors that contribute to the excited-state acidities of hydroxyl aromatic compounds and construct an effective descriptor that yields excited-state acidity of photoacids based on simple TDDFT calculations.

2 Computational details

A total of 14 hydroxyl photoacids were investigated in this work. We optimized the ground and S_1 excited-state geometries of the selected molecules by utilizing density functional theory (DFT)[33–35] and time dependent density functional theory (TDDFT),[33–40] respectively. The ωB97X-D exchange–correlation functional[41] and the 6-31G(d) basis set[42–47] are used for these calculations. Compared to the B3LYP functional applied in Liu and Pedersen's work,[32] the ωB97X-D[41] functional includes the long-range exchange correlation and dispersion terms that might be important for the selected excited-state systems. We have performed similar calculations using the B3LYP and CAM-B3LYP[48] functionals (see the ESI,† Fig. S1), which show that ωB97X-D results in a slightly better performance in the correlation between the MEP and pK_a*. In addition, since there is no significant long-range interaction as we only focus on the intramolecular properties of a single photoacid molecule rather than the acid–base pair in this study, the 6-31G(d) basis set is selected. We have also tested the basis set dependence, and it is found that the 6-31G(d) basis set is sufficient to give consistent MEP values. The Gaussian09 quantum chemistry package suite[49] is used for all the calculations reported in this work.

After structure optimizations, single point calculations were carried out to obtain the local molecular electrostatic potentials at the proton-donating oxygen atom for the S_0 and S_1 states. The molecular electrostatic potential at the position of nucleus A (R_A) is defined as[50,51]

$$\phi_A(R_A) = \sum_{B \neq A} \frac{Z_B}{|R_A - R_B|} - \int \frac{\rho(r)}{|R_A - r|} dr, \qquad (1)$$

where Z_B is the atomic number of nucleus B, and $\rho(r)$ is the electron density at position r. Note that the contribution from nucleus A itself is removed to avoid Coulomb divergence. Because the calculations reported in this work concern the same oxygen atomic center as nucleus A, removing the contribution from the oxygen nuclear charge amounts to a constant shift in the calculated MEP, and thus it does not affect the analysis presented in this work. All single point calculations were also carried out at the TDDFT ωB97X-D/6-31G(d) level of theory. In the single point calculation, the electron density on the integration grids can be obtained by either DFT or TDDFT. Using the electron density on grids, the second term in eqn (1) can be numerically evaluated and the MEP is obtained while the first term is trivial to determine once the positions of the nuclei are determined. In addition, population analysis as implemented in the Gaussian09 package suite is used in single point calculations to obtain the atomic charges in our comparative studies.

In addition to the DFT calculations in vacuum, the Polarizable Continuum Model (PCM)[52–55] implemented in the Gaussian09 package was also applied to take solvent effects into account. A series of solvent conditions with dielectric constants ranging from low to high were used: cyclohexane, dichloromethane, tetrahydrofuran (THF), ethanol, methanol, and water solvents were modeled. The optimization calculations for 14 photoacids were carried out with each PCM model in both the S_0 and S_1 states. For ground states, frequency analysis was performed on each optimized structure to ensure the quality of the structure optimization. For excited states, the stationary geometries were carefully checked by having their maximum force, RMS force, RMS displacement, and RMS displacement converged under the Gaussian09 default threshold in the SCF iteration processes. By utilizing the optimized structures, single point calculations with PCM models were applied to obtain ϕ_O and ϕ_O^* under different solvent conditions. In the next section, we will first present the results in vacuum and then investigate the MEP changes due to the solvent effects.

3 Results and discussion

3.1 Ground state pK_a–MEP relationship

We first investigate 12 mono-hydroxyl substituted aromatic compounds with previously reported ground state and excited state acid dissociation constants. The chemical structures and labels for these molecules are shown in Fig. 1, and they can be divided into three different classes. Compounds **a–g** are phenol derivatives with methyl-, bromo-, methoxy- and cyano-functional groups substituted at different positions. Compounds **h–j** are naphthol derivatives that contain two aromatic rings. Compounds **k** and **l** are both hydropyrene derivatives that exhibit the most expanded aromatic system (4 rings) in this study. These molecules represent a wide range of hydroxyl aromatic compounds that have found broad applications as photoacids. Note that we focus on hydroxyl compounds because they are among the most well-studied photoacids and their excited-state pK_a* values are available in the literature. Other N- or S-containing compounds have also exhibited strong excited-state acidities. However, since generally speaking the experimental pK_a* data are only available for a few of these non-hydroxyl photoacids, we will only consider the hydroxyl compounds in this study.

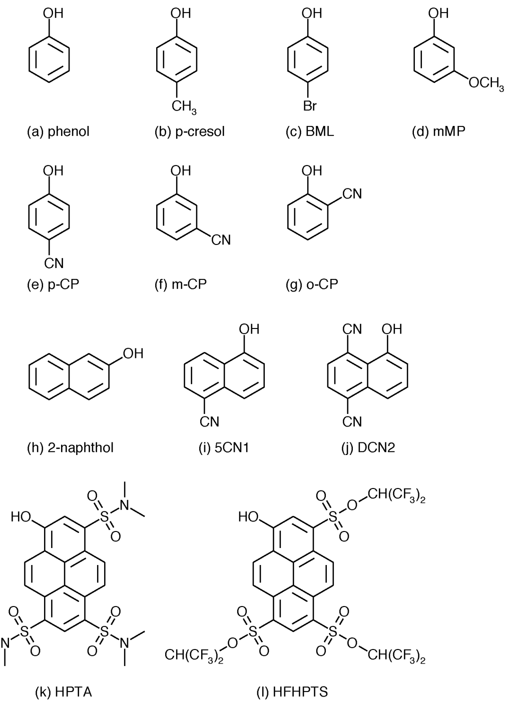

(a) phenol (b) p-cresol (c) BML (d) mMP

(e) p-CP (f) m-CP (g) o-CP

(h) 2-naphthol (i) 5CN1 (j) DCN2

(k) HPTA (l) HFHPTS

Fig. 1 Mono-hydroxyl substituted aromatic photoacids.

Table 1 lists the measured pK_a and pK_a* values of the selected compounds. The experimental excited-state acidities for these model compounds were obtained in an aqueous environment either by fluorescence titration or by Förster cycle methods (see references listed in Table 1). Notably, the phenol derivatives generally exhibit larger pK_a and pK_a* values than those of both the naphthol and hydropyrene derivatives, because the extended aromatic rings for either naphthol or hydropyrene derivatives may stabilize the conjugated bases of these species, which leads to stronger acidities in either the ground or the excited state.

To confirm the validity of utilizing MEP as a descriptor of acidity and to justify the level of theory used in this work for the selected model compounds, we first investigate the pK_a–MEP relationship in the ground states. To this end, the ground state MEP values on the oxygen atom of the acidic hydroxyl group, ϕ_O, of these molecules under vacuum conditions are calculated and compared with the experimental pK_a value (see Fig. 2 and the ESI,† Table S1). Clearly, the ground state MEP on the hydroxyl oxygen atom exhibits a strong linear correlation with pK_a (R^2 = 0.9235). The results are in good agreement with Liu and Pedersen's work,[32] although different functional and basis sets are used for the MEP calculations in our work. The linear relationship between ϕ_O and pK_a provides an quantitative scale to estimate acidity. Moreover, the excellent correlation also indicates that the level of theory utilized in this study is sufficient to describe the acidity dependence on the environmental electrostatic effect.

The relation between the molecular acidity and MEP on the proton-donating atom can be interpreted in a microscopic

Table 1 Experimental ground state and excited state acidities

Compound	pK_a	pK_a*	Ref.
a	10.0	4.0	11
b	10.26	4.3	1 and 11
c	9.36	3.1	1 and 11
d	9.65	4.6	1 and 11
e	7.74	3.33	12
f	8.34	1.89	12
g	6.97	0.66	12
h	9.5	3.1	1 and 56
i	8.5	−2.8	14 and 15
j	7.8	−4.5	14 and 57
k	5.6	−1.0	58
l	4.4	−3.9	58

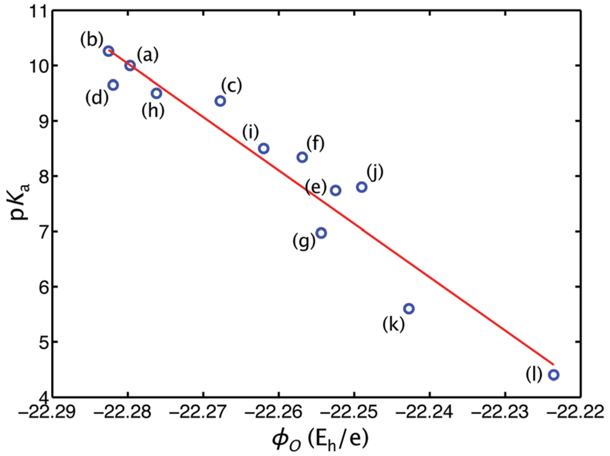

Fig. 2 Correlation between the ground state acidity and the calculated MEP on the oxygen atom of the hydroxyl group under vacuum conditions. Points are labeled according to Fig. 1. The best linear regression to the dataset is $y = -96.7{\cdot}x - 2.1435 \times 10^3$, with $R^2 = 0.9235$.

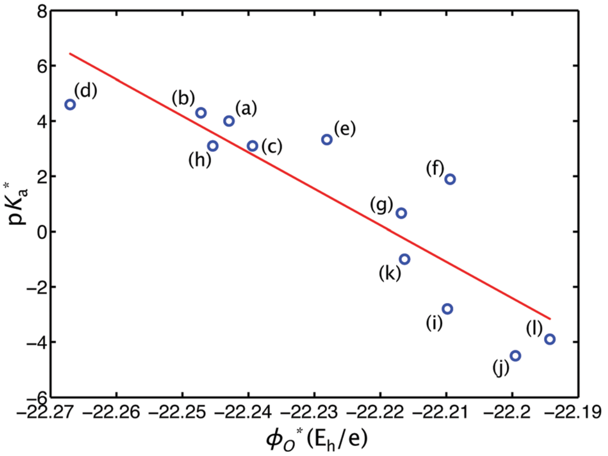

Fig. 3 Correlation between the excited state acidity and the calculated S_1 excited-state MEP on the oxygen atom of the hydroxyl group under vacuum conditions. Points are labeled according to Fig. 1. The best linear regression to the dataset is $y = -132.0{\cdot}x - 2.9321 \times 10^3$, with $R^2 = 0.7785$.

picture of proton dissociation, in which the proton transfer is highly dependent on molecular electrostatic interactions. The electrostatic potential at the acidic site thus reflects the electrostatic influence of the local environments relevant to proton dissociation. When the chemical structure is modified by the addition of electron withdrawing/donating groups or the dielectricity of the environment, the electron density of the O–H bond changes due to the electrostatic force acting on it, leading to changes in the local MEP at the position of the oxygen atom. As a result, the MEP on the oxygen atom measures the electron density between the oxygen atom and the proton, which is strongly correlated with the strength of the chemical bond between the proton and the proton-donating atom, and hence the molecular acidity. Therefore, if the MEP on the proton-donating atom becomes more negative (positive) as the bond electron density increases (decreases), the compound is expected to become a weaker (stronger) acid. This principle should be applicable to molecules in the excited states as well.

3.2 Excited state pK_a*–MEP relationship

Now we turn to investigate the excited-state acidities. From Table 1, the pK_a* values of these hydroxyl photoacids range from −7 to 4.6. Compared to the ground-state acidities, the acidities in the excited states are enhanced by up to five orders of magnitude upon photoexcitation. It was suggested that the intramolecular charge transfer from the proton-donating atom to the conjugated ring system upon photoexcitation decreases the electron density on the hydroxyl group, leading to a much stronger acidity in the excited state.[10] The change of the partial charge upon excitation can be clearly seen in the ESI,† Table S2, in which the Mulliken and Hirshfeld charges on the proton-donating oxygen of the photoacids are listed. It is shown that the partial charge on the hydroxyl oxygen systematically decrease upon excitation. This charge transfer character of the S_1 excited state is critical for the enhanced acidities of hydroxyl aromatic photoacids, and the shift in electron density should reflect on the change in the MEP. To examine the correlation between the excited state MEP and the excited state acidities, we calculate ϕ_O* under vacuum conditions and correlate the results with the experimental pK_a* values (Fig. 3).

Fig. 3 shows the clear correlation between ϕ_O* and the corresponding experimental pK_a* value ($R^2 = 0.7785$). The correlation is not as high as that in the ground states, nevertheless it shows that ϕ_O* is an adequate descriptor for excited-state acidities. To examine the DFT functional dependence, we have also calculated ϕ_O* using the B3LYP and CAM-B3LYP methods. The ϕ_O*–pK_a* correlations of these two alternative DFT functionals are provided in the ESI,† Fig. S1, which shows that the ωB97X-D functional yields a slightly better correlation than the ones obtained by either B3LYP or CAM-B3LYP. Thus the level of our TDDFT calculations can be justified. The linear regression equation provides a simple way to estimate the excited-state acidity for hydroxyl-substituted photoacids with simple TDDFT calculations. Notably, the linear relation that correlates pK_a* to ϕ_O* is different from the one obtained in the ground state (Fig. 2). Compared to the ground-state pK_a–MEP relationship, the slope of the linear regression in the excited state appears to be much steeper, indicating an enhanced sensitivity of pK_a* to the MEP on the proton-donating atom. It has been reported that the polarizability of aromatic molecules may increase upon excitation,[59–61] leading to more substantial changes in the electron density distribution in response to the environmental electrostatic interactions. Thus the excited states show a different pK_a*–MEP relationship.

More importantly, MEP correctly predicts the trends of acidity changes upon photoexcitation, making it a useful descriptor for pK_a* in the excited states for the class of hydroxyl aromatic photoacids studied here. For example, **p-CP** (compound **e**) and **m-CP** (compound **f**) show distinct photoacidity behavior. In the ground state, **p-CP** is more acidic than **m-CP** due to the resonance effect which stabilizes the resonance structure of the conjugate base of **p-CP**. On the other hand, in the S_1 state, the intramolecular charge transfer upon excitation from the hydroxyl group to the aromatic ring will enhance the inductive effect of the electron-withdrawing cyano-group, turning **m-CP** into a stronger acid than **p-CP** in the excited state[12] (see Table 1). In our calculations, the MEP at the proton-donating site of **p-CP** in the ground state is less negative than that of **m-CP**, reflecting less electron density on the oxygen atom in **p-CP**, and hence the stronger acidity of **p-CP**. However, in the S_1 excited state, the MEP at the proton-donating site of **p-CP** becomes more negative than that of **m-CP**, predicting a weaker acidity in **p-CP** (ESI,† Tables S1 and S3). Therefore, the theoretical MEP values capture the electronic effects and correctly predict the order of acidity for **p-CP** and **m-CP** both in the ground and excited states. Our results demonstrate that using MEP as an acidity descriptor is valid not only in the ground states but also in the excited states for hydroxyl aromatic photoacids.

Considering that alternative descriptors for ground-state acidity have been proposed previously, it is of interest to compare the performance of the MEP descriptor emphasized in this work to other methods. To this end, we have examined the correlations between the acidity and the Mulliken charge on the oxygen atom, the Hirshfeld charge on the oxygen atom, the O–H bond length, and the C–O bond length. For the same set of model hydroxyl compounds, these descriptors exhibit reasonable correlations with the ground-state acidity (ESI,† Fig. S3). However, when the correlations in the excited states are examined, it is clear that these descriptors do not describe the excited-state acidities at all (Fig. 4). This is in stark contrast to the performance of the MEP-based descriptor. Notably, the atomic partial charges on the proton-donating oxygen atom do not seem to capture the trend in excited-state acidity as the MEP indicator does. This result is unexpected, and we suspect that the MEP has more long-range contributions and therefore provides a better description of the local electrostatic environment for proton transfer. Thus, the MEP at the proton-donating nucleus clearly is a more effective descriptor for the photoacidity of hydroxyl chromophores.

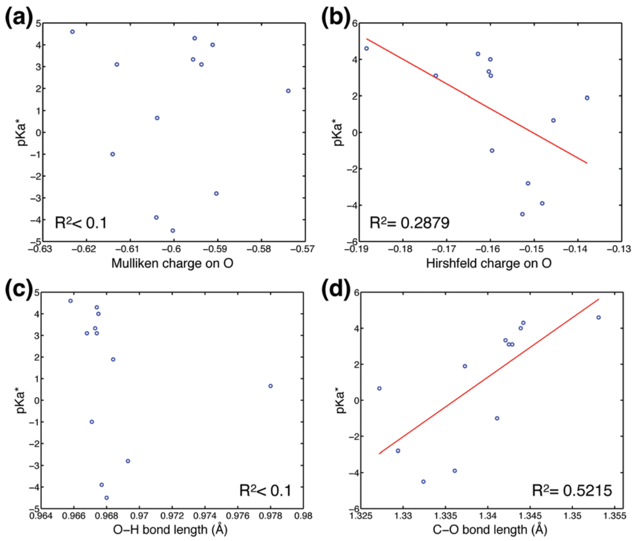

Fig. 4 Correlations between the excited-state acidity and various theoretical acidity descriptors proposed previously: (a) Mulliken charge on the oxygen atom of the hydroxyl group, (b) Hirshfeld charge on the oxygen atom of the hydroxyl group, (c) the O–H bond length, (d) the C–O bond length.

3.3 pK_a* of charged species and MEP difference

In addition to the neutral compounds listed in Fig. 1, we have also examined two positively charged photoacids (see Fig. 5) in order to expand the chemical scope of using MEP on the proton-donating atom as a quantum descriptor for excited-state acidities. The question is to see whether or not the pK_a* of these charged species could be described by the same pK_a*–MEP relationship as the one obtained from the neutral species (Fig. 3). The results are depicted in the ESI,† Fig. S2 and Table S3. Notably, while the neutral molecules have MEP values ranging from −22.15 to −22.3, the positively-charged trimophonium cation and **NM6HQ+** exhibit distinct behaviors (see the ESI,† Table S3 and Fig. S2). These two cations show strongly positive MEP at the proton-donating site under vacuum conditions which may be attributed to the positive charge on nitrogen in their chemical structures. Because of the extra positive charge, the electron density on the hydroxyl group is significantly reduced through the resonance with the aromatic rings. As a result, the electrostatic potential on the hydroxyl oxygen becomes much more positive than those in neutral molecules. It is important to note that the linear relations between MEP and pK_a for different types of molecules in the ground states are different.[32] For excited state acidities, the deviation of the correlations with MEP for different types of molecules (neutral or positive here) should be expected.

The different dependences of acidity on MEP at the proton-donating atom seem to limit the usefulness of MEP as a descriptor of excited-state acidities. Nevertheless, for ground state systems, Liu and Pedersen[32] have shown that a universal linear relationship can be constructed to provide acidity measures over wide varieties of compounds through considering the difference in the MEP values relative to that of the bare atoms. Inspired by their work, we seek to explore an generalized descriptor for the excited state acidities that could unify the neutral and cationic pK_a* data. To this end, we propose to consider the differences in the pK_a* and MEP values relative to those of the ground state values, *i.e.* $\Delta pK_a = pK_a^* - pK_a$ and $\Delta\phi_O = \phi_O^* - \phi_O$, as an effective descriptor of excited state acidity for both the neutral and positive charged species. By subtracting the ground-state pK_a and ϕ_O values from the excited-state

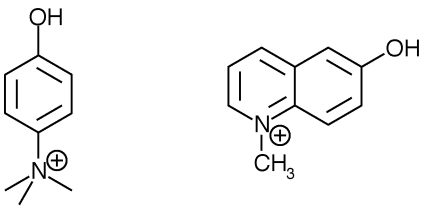

(m) Trimophonium cation (n) NM6HQ+

Fig. 5 Positively-charged mono-hydroxyl substituted photoacids studied in this work.

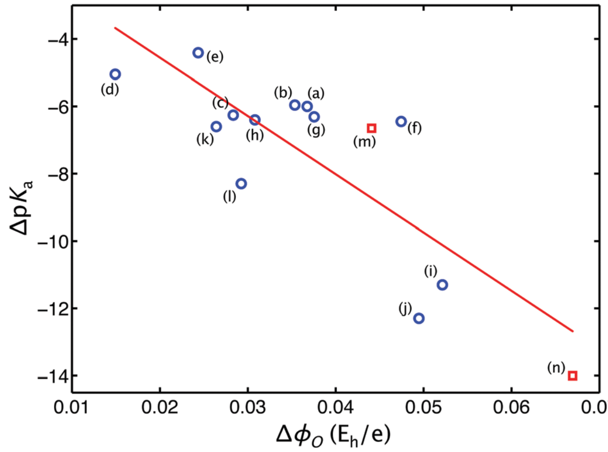

Fig. 6 Correlations between ΔpK_a and ΔMEP for both the neutral (blue circles) and positively-charged (red squares) hydroxyl photoacids. Points are labeled according to Fig. 1 and 5. The best linear regression to the dataset is $y = -173.0804 \cdot x - 1.0943$, with $R^2 = 0.6630$.

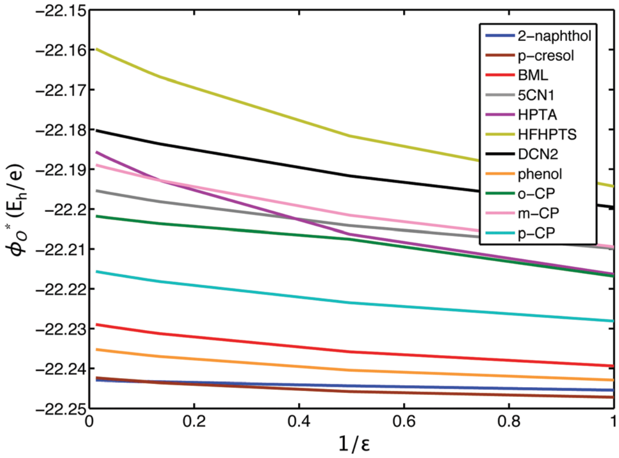

Fig. 7 The excited state MEP on the hydroxyl oxygen atom (ϕ_O*) as a function of the inverse dielectric constant.

pK_a* and ϕ_O*values respectively, we aim to focus on the effects of photoexcitation. Note that since the ground state acidities for organic compounds are often readily available, the difference in values can be easily obtained. Fig. 6 shows the correlation plot of the two difference values for all 14 compounds investigated in this work, and a reasonable correlation between ΔpK_a and $\Delta\phi_O$ can be clearly seen. It is remarkable that after the correction, the points for the two cationic photoacids fall in line with that of the neutral species. The contribution of the positive charge to the electron density distribution in the trimophonium cation and **NM6HQ+** is removed by the correction, leaving only the electronic excitation that perturbs the MEP and acidity of the system. Thus, the description for neutral and positively charged photoacids can be integrated as one to give a generalized estimation of the acidity change due to excitation. The possibility to describe the excited-state acidities of hydroxyl aromatic compounds in a universal relationship indicates the generality of the MEP-based descriptor for excited-state acidity and that a universal descriptor for excited-state acidities covering compounds with a variety of chemical structures could be established.

3.4 Solvent effects on photoacidity

Since the excited-state acidity strongly depends on the solvent[14] and the acidity is an important factor in the selection of photoacids in various applications, solvent effects should play important roles in the effectiveness of photoacids. Here, we investigate the solvent effects in excited-state acidity by carrying out TDDFT calculations with the PCM model in a series of solvent environments ranging from low polarity to high polarity. The solvent dependences of ϕ_O* for different compounds are shown in Fig. 7 and in the ESI,† Table S4, and the dielectric screening effect can be clearly observed. Note that with the increase of solvent dielectricity, the screening effects should be enhanced, and hence the oxygen atom on the hydroxyl group should exhibit a less negative electrostatic potential. From the ESI,† Table S4, it is clear that in most cases, ϕ_O* does increase with the higher dielectric constant of the environment, except for mMP, the trimophonium cation and **NM6HQ+**. These three species, including the two cations investigated in the previous paragraph, exhibit a minor negative dielectric constant dependence that is opposite that of the other compounds. We believe that this opposite effect can be attributed to the screening of the positive charge on the molecular skeleton. For mMP, which is in the neutral state, its relatively small dipole compared to the other hydroxyl photoacids may result in poor sensitivity to the dielectric environment, and its MEP dependence on the dielectric constant is negligible. Hence, the three data points are excluded from Fig. 7.

The molecular acidity should be enhanced in solvents with larger dielectric constants,[62] which is described by the MEP at the proton-donating atom (ϕ_O*). The MEP based pK_a* descriptor we proposed here correctly captures the dielectricity induced acidity change (Fig. 7). Due to the negative linear correlation between ϕ_O* and pK_a*, the increased ϕ_O* in stronger dielectric environments for most of the molecules we examined in this work represents increased acidities. With the use of ϕ_O* as a pK_a* descriptor, the strength of the solvent effects on the excited state acidity can be estimated. It will be interesting to compare our results to the experimental data quantitatively, especially for the three compounds whose MEP descriptor predicts an opposite solvent dielectric dependence. However, the experimental solvent-dependent pK_a* values for these compounds are not available.

Furthermore, Fig. 7 shows that the solvent induced MEP changes are relatively small compared to the MEP differences between species, and the dependence of MEP on solvent dielectricity for different compounds exhibit similar slopes. As a result, the relative MEP values of different chemical species exhibit only a weak solvent dependence. To further quantify the strengths of the solvent effects on MEP, we assume that the MEP changes in Fig. 7 share a universal simple dielectric screening effect. Thus, the ϕ_O* in different solvents should then be described by

$$\phi_O{}^*(\varepsilon_i) = \phi_0{}^*(\varepsilon_i = \varepsilon_0) + \alpha\left(\frac{1}{\varepsilon_i} - \frac{1}{\varepsilon_0}\right), \qquad (2)$$

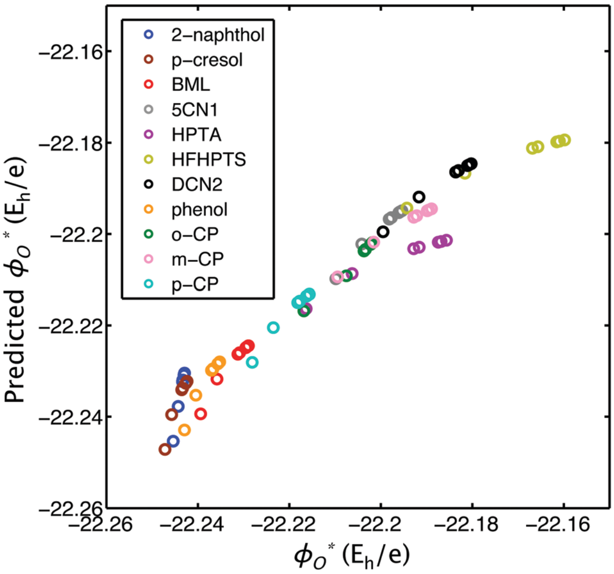

Fig. 8 Relationship between the predicted $\phi_O{}^*(\varepsilon_i)$ obtained by eqn (2) and $\phi_O{}^*$ calculated by DFT with implicit solvent models.

where $\phi_0{}^*(\varepsilon_i = \varepsilon_0)$ is the $\phi_O{}^*$ obtained under vacuum conditions, ε_0 is the vacuum dielectric constant, and α is a screening factor representing the common solvent effects on MEP shared by all the examined photoacids. By linear fitting of eqn (2) to the data shown in Fig. 7 (also in ESI,† Table S4), α is determined to be about -0.0151. We then obtain a simple relationship to quantify the value of MEP at different solvent dielectricities. In other words, the determination of the excited-state pK_a* value only requires the MEP value calculated in vacuum.

To confirm the effectiveness of eqn (2), we calculated the estimated solvent-dependent $\phi_O{}^*$ for each molecule in different solvents by utilizing $\phi_O{}^*$ obtained under vacuum conditions and eqn (2). The comparison of these predicted MEP values with the ones calculated by TDDFT with PCM implicit solvent models is shown in Fig. 8, which clearly shows that eqn (2) provides an accurate estimation of the solvent-dependent MEP on the proton-donating atom. If only a continuous solvation model is considered, the solvent screening effects on $\phi_O{}^*$ can be easily determined, therefore DFT calculations under vacuum conditions are sufficient to provide an effective quantum descriptor for the excited-state acidities.

In summary, the excited state acidities and $\phi_O{}^*$ exhibit a strong linear correlation, providing us with an relatively efficient theoretical pK_a* descriptor compared to thermodynamic calculations. The MEP based pK_a* descriptor can effectively predict the trends of acidity changes upon photoexcitation. Furthermore, the regression equation can be generalized to give descriptions of both the neutral and positively charged photoacids, by applying the ground state MEP and experimental ground state pK_a values as correction terms. The solvent effects on molecular acidity are included by utilizing the implicit solvent model. The dielectricity induced acidity change can be observed not only for ground state acids, but also for the photoacid category by applying the MEP based pK_a* descriptor we developed here. With eqn (2), the strength of the dielectric effects on MEP is quantified, which provides us with an efficient means to predict the photoacidity in different solvents. Finally, we note that explicit solvent effects such as hydrogen-bond interactions and micro-solvation environments are not included in our calculations, and they could play a significant part in the excited-state acidities.

4 Conclusions

In this work, we investigated a series of neutral aromatic hydroxyl-substituted photoacids to reveal the strong linear correlation between the measured excited state acidities and molecular electrostatic potentials on the proton-donating atom calculated using the ωB97X-D[41]/6-31G(d) level of TDDFT theory in vacuum. In addition, we showed that the MEP based pK_a* descriptor correctly reproduces the trends in the substituent and ring-size effects for the photoacids studied in this work. Moreover, we have also studied two additional photoacids that are positively-charged. Compared to the neutral hydroxyl photoacids, these two compounds exhibit different pK_a* dependences on MEP; however, when we consider the differences in the excited-state pK_a* and MEP values relative to those of the ground states, both the neutral and positively-charged photoacids exhibit the same linear ΔpK_a*–ΔMEP relationship. The linear correlation provides us with an efficient quantitative descriptor to estimate the pK_a* values of hydroxyl photoacids using simple TDDFT calculations. Note that the number of compounds studied in this work (14 molecules) is limited by the availability of experimental data on the excited-state pK_a* values. Although the size of the database studied here is not as satisfactory as we would like to have, we believe that the trend and correlation are clearly demonstrated to make the MEP on the proton-donating atom a useful indicator for the photoacidity of hydroxyl chromophores.

In addition to the DFT calculations in vacuum, we have also carried out calculations with the PCM solvation model for several solvent environments. With the solvent effect taken into account, the strong linear correlation still holds, and we showed that the solvent-dependent changes in MEP on the proton-donating atom can be described by a simple dielectric solvation expression. As a result, we demonstrate that the vacuum MEP values can be used to estimate the excited-state pK_a* values under different solvent conditions, indicating that the contribution of solvent screening effects on the electron density distribution determines the pK_a* changes of the photoacids.

Significant efforts have been invested to understand the mechanisms of photoacidity and excited state proton transfer in chromophores. The pK_a* values in the molecular excited states are critical for the effectiveness of photoacids in organic synthetic processes as well as the mechanisms of excited-state proton transfer reactions. Therefore, our results should have important implications for the design of photoacids and the study of excited-state proton transfer reactions. The linear relation between the MEP on the proton-donating atom and pK_a* could be very useful for the studies of photoacids. The simple quantum descriptor for pK_a* based on MEP would enable a fast screening of chemical structures so that the photoacids suitable for specific photoacid generators for photolithography or photoinitiators for catalytic polymerization reactions can be efficiently selected without performing costly experiments.

Furthermore, we believe that the molecular electrostatic potential on the proton-donating atom directly reflects the impact of environmental interactions on the O–H bond and serves as an appropriate measuring scale of acidity. This measuring scale, which has been shown to be successful for ground state acidity in the literature,[32] is demonstrated to also be valid in the excited-state systems in this study. It is remarkable that a simple MEP value can capture system-dependent $\mathrm{p}K_a{}^*$ reasonably well. We believe that our work also reveals significant physical insights towards the understanding of molecular acidity.

The confirmation of MEP as an effective quantum descriptor for molecular acidity in the excited states lends strong support to the model that electrostatic interactions and electron density changes to the proton-donating atom determines the acidity of a molecular system. It is interesting to note that the acidity is determined by the free energy difference between the protonated- and deprotonated molecular states, and it should be a complex chemical property that depends on many system variables, for example, the O–H bond dissociation energy, bond polarizability, solvent environment, and stability of the deprotonated species. Nevertheless, these factors affecting acidity also contribute to the changes in the value of the molecular electrostatic potential at the position of the proton-donating atom. Our results might imply that the electrostatic interactions dominate proton transfer in acid–base reactions both in the ground and excited states of molecular acids. In particular, for hydroxyl-substituted aromatic molecules, it was shown that the charge-transfer (CT) character of the excited state plays a key role in driving the proton transfer reactions in the excited state.[18] Our calculations indicate that the CT character could be described by the MEP at the proton-donating atom, which is effective for measuring the local CT effect at the position. In addition, our results also imply that the entropic effect at most plays only a minor role in determining the $\mathrm{p}K_a{}^*$ value for the systems studied in this work.

Finally, we note that the correlation revealed in this research is specific to mono-hydroxyl-substituted photoacids. Investigations on *N*- or *S*-substituted photoacids are currently work in progress. According to the ground state study by Liu and Pedersen, we expect that photoacids with different proton-donating atoms will show a distinct $\mathrm{p}K_a{}^*$–MEP relationship; nevertheless, there remains a possibility that a universal scale might exist to describe the excited-state acidities of different types of photoacids on the same footing.

Conflicts of interest

There are no conflicts to declare.

Acknowledgements

YCC acknowledges the Ministry of Science and Technology, Taiwan (Grant No. NSC 105-2113-M-002-012), the National Taiwan University (Grant No. 103R891305), and the Center for Quantum Science and Engineering (Subproject: 103R891401) for financial support. We are grateful to the Computer and Information Networking Center, National Taiwan University for the support of high-performance computing facilities. We are grateful to the National Center for High-performance Computing for the computer time and facilities.

References

1 E. L. Wehry and L. B. Rogers, *Spectrochim. Acta*, 1965, **21**, 1976.
2 J. F. Ireland and P. A. H. Wyatt, *Adv. Phys. Org. Chem.*, 1976, **12**, 131.
3 R. M. D. Nunes, M. Pineiro and L. G. Arnaut, *J. Am. Chem. Soc.*, 2009, **131**, 9456.
4 C. E. M. Carvalho, A. S. Silva, I. M. Brinn, A. V. Pinto, M. C. F. R. Pinto, S. Lin, T. A. Moore, D. Gust and M. Maeder, *Phys. Chem. Chem. Phys.*, 2002, **4**, 3383.
5 S. G. M. Portugal, L. A. Montero-Cabrera, L. A. Diaz and I. M. Brinn, *J. Photochem. Photobiol., A*, 2006, **181**, 370.
6 M. Shirai and M. Tsunooka, *Prog. Polym. Sci.*, 1996, **21**, 1.
7 C. Fu, J. Xu and C. Boyer, *Chem. Commun.*, 2016, **52**, 7126.
8 G. M. Wallraff and W. D. Hinsberg, *Chem. Rev.*, 1999, **99**, 1801.
9 P. Shum, J.-M. Kim and D. H. Thompson, *Adv. Drug Delivery Rev.*, 2001, **53**, 273.
10 G. Granucci, J. T. Hynes, P. Millié and T. H. Tran-Thi, *J. Am. Chem. Soc.*, 2000, **122**, 12243.
11 E. L. Wehry and L. B. Rogers, *J. Am. Chem. Soc.*, 1965, **87**, 4234.
12 S. G. Schulman, W. R. Vincent and W. J. M. Underberg, *J. Phys. Chem.*, 1981, **85**, 4068.
13 N. Agmon, W. Rettig and C. Groth, *J. Am. Chem. Soc.*, 2002, **124**, 1089.
14 C. Spies, S. Shomer, B. Finkler, D. Pines, E. Pines, G. Jung and D. Huppert, *Phys. Chem. Chem. Phys.*, 2014, **16**, 9104.
15 E. Pines, D. Pines, T. Barak, B.-Z. Magnes, L. M. Tolbert and J. E. Haubrich, *Ber. Bunsen-Ges. Phys. Chem.*, 1998, **102**, 511.
16 H. Ihmels and K. Schafer, *Photochem. Photobiol. Sci.*, 2009, **8**, 309.
17 D. Huppert, L. M. Tolbert and S. Linares-Samaniego, *J. Phys. Chem. A*, 1997, **101**, 4602.
18 N. Agmon, *J. Phys. Chem. A*, 2005, **109**, 13.
19 T. Förster, *Z. Elektrochem.*, 1950, **54**, 531.
20 A. Weller, *Z. Elektrochem.*, 1952, **56**, 662.
21 W. Bartok, P. J. Lucchesi and N. S. Snider, *J. Am. Chem. Soc.*, 1962, **84**, 1842.
22 A. J. Kirby, *Adv. Phys. Org. Chem.*, 1994, **29**, 87.
23 R. D. Amos, N. C. Handy, P. G. Jones, A. J. Kirby, J. K. Parker, J. M. Percy and M. D. Su, *J. Chem. Soc., Perkin Trans. 2*, 1992, 549.
24 J. E. Davies, N. L. Doltsinis, A. J. Kirby, C. D. Roussev and M. Sprik, *J. Am. Chem. Soc.*, 2002, **124**, 6594.
25 B. G. Tehan, E. J. Lloyd, M. G. Wong, W. R. Pitt, J. G. Montana, D. T. Manallack and E. Gancia, *Quant. Struct.-Act. Relat.*, 2002, **21**, 457.

26 U. A. Chaudry and P. L. A. Popelier, *J. Org. Chem.*, 2004, **69**, 233.

27 S. E. O'Brie and P. L. A. Popelier, *J. Chem. Inf. Comput. Sci.*, 2001, **41**, 764.

28 C. Grüber and V. Buß, *Chemosphere*, 1989, **19**, 1595.

29 M. J. Citra, *Chemosphere*, 1999, **38**, 191.

30 K. R. Adam, *J. Phys. Chem. A*, 2002, **106**, 11963.

31 R. Ponec, L. Amat and R. Carbó-Dorca, *J. Phys. Org. Chem.*, 1999, **12**, 447.

32 S. Liu and L. G. Pedersen, *J. Phys. Chem. A*, 2009, **113**, 3648.

33 P. Hohenberg and W. Kohn, *Phys. Rev.*, 1964, **136**, B864.

34 W. Kohn and L. J. Sham, *Phys. Rev.*, 1965, **140**, A1133.

35 R. G. Parr and W. Yang, *Density-functional theory of atoms and molecules*, Oxford University Press, New York, 1994.

36 R. Bauernschmitt and R. Ahlrichs, *Chem. Phys. Lett.*, 1996, **256**, 454.

37 C. V. Caillie and R. D. Amos, *Chem. Phys. Lett.*, 1999, **308**, 249.

38 C. V. Caillie and R. D. Amos, *Chem. Phys. Lett.*, 2000, **317**, 159.

39 F. Furche and R. Ahlrichs, *J. Chem. Phys.*, 2002, **117**, 7433.

40 G. Scalmani, M. J. Frisch, B. Mennucci, J. Tomasi, R. Cammi and V. Barone, *J. Chem. Phys.*, 2006, **124**, 094107.

41 J. D. Chai and M. Head-Gordon, *Phys. Chem. Chem. Phys.*, 2008, **10**, 6615.

42 R. Ditchfield, W. J. Hehre and J. A. Pople, *J. Chem. Phys.*, 1971, **54**, 724.

43 W. J. Hehre, R. Ditchfield and J. A. Pople, *J. Chem. Phys.*, 1972, **56**, 2257.

44 M. M. Francl, W. J. Pietro, W. J. Hehre, J. S. Binkley, M. S. Gordon, D. J. DeFrees and J. A. Pople, *J. Chem. Phys.*, 1982, **77**, 3654.

45 V. A. Rassolov, M. A. Ratner, J. A. Pople, P. C. Redfern and L. A. Curtiss, *J. Comput. Chem.*, 2001, **22**, 976.

46 P. C. Hariharan and J. A. Pople, *Theor. Chim. Acta*, 1973, **28**, 213.

47 M. J. Frisch, J. A. Pople and J. S. Binkley, *J. Chem. Phys.*, 1984, **80**, 3265.

48 T. Yanai, D. P. Tew and N. C. Handy, *Chem. Phys. Lett.*, 2004, **393**, 51.

49 M. J. Frisch, G. W. Trucks, H. B. Schlegel, G. E. Scuseria, M. A. Robb, J. R. Cheeseman, G. Scalmani, V. Barone, B. Mennucci, G. A. Petersson, H. Nakatsuji, M. Caricato, X. Li, H. P. Hratchian, A. F. Izmaylov, J. Bloino, G. Zheng, J. L. Sonnenberg, M. Hada, M. Ehara, K. Toyota, R. Fukuda, J. Hasegawa, M. Ishida, T. Nakajima, Y. Honda, O. Kitao, H. Nakai, T. Vreven, J. A. Montgomery, Jr., J. E. Peralta, F. Ogliaro, M. Bearpark, J. J. Heyd, E. Brothers, K. N. Kudin, V. N. Staroverov, R. Kobayashi, J. Normand, K. Raghavachari, A. Rendell, J. C. Burant, S. S. Iyengar, J. Tomasi, M. Cossi, N. Rega, J. M. Millam, M. Klene, J. E. Knox, J. B. Cross, V. Bakken, C. Adamo, J. Jaramillo, R. Gomperts, R. E. Stratmann, O. Yazyev, A. J. Austin, R. Cammi, C. Pomelli, J. W. Ochterski, R. L. Martin, K. Morokuma, V. G. Zakrzewski, G. A. Voth, P. Salvador, J. J. Dannenberg, S. Dapprich, A. D. Daniels, O. Farkas, J. B. Foresman, J. V. Ortiz, J. Cioslowski and D. J. Fox, *Gaussian 09, Revision A.02*, Gaussian, Inc., Wallingford CT, 2009.

50 B. G. Johnson, P. M. W. Gill., J. A. Pople and D. J. Fox, *Chem. Phys. Lett.*, 1993, **206**, 239.

51 V. Dimitrova, S. Ilieva and B. Galabov, *J. Mol. Struct.: THEOCHEM*, 2003, **637**, 73.

52 J. Tomasi, B. Mennucci and R. Cammi, *Chem. Rev.*, 2005, **105**, 2999.

53 M. Cossi and V. Barone, *J. Chem. Phys.*, 2001, **115**, 4708.

54 M. Cossi, N. Rega, G. Scalmani and V. Barone, *J. Comput. Chem.*, 2003, **24**, 669.

55 B. Mennucci, E. Cancès and J. Tomasi, *J. Phys. Chem. B*, 1997, **101**, 10506.

56 R. Boyer, G. Deckey, C. Marzzacco, M. Mulvaney, C. Schwab and A. M. Halpern, *J. Chem. Educ.*, 1985, **62**, 630.

57 L. M. Tolbert and J. E. Haubrich, *J. Am. Chem. Soc.*, 1994, **116**, 10593.

58 B. Finkler, C. Spies, M. Vester, F. Walte, K. Omlor, I. Riemann, M. Zimmer, F. Stracke, M. Gerhards and G. Jung, *Photochem. Photobiol. Sci.*, 2014, **13**, 548.

59 M. Ponder and R. Mathies, *J. Phys. Chem.*, 1983, **87**, 5090.

60 H. K. Sinha, P. C. P. Thomson and K. Yates, *Can. J. Chem.*, 1990, **68**, 1507.

61 S. Ferdous and J. B. Lagowski, *J. Polym. Sci., Part B: Polym. Phys.*, 2007, **45**, 1983.

62 D. Pines, S. Keinan, P. M. Kiefer, J. T. Hynes and E. Pines, *J. Phys. Chem. B*, 2015, **119**, 9278.